Microbiota-mediated nitrogen fixation and homeostasis in aerial root-mucilage

Pang Zhiqiang
Xishuangbanna Tropical Botanical Garden, Chinese Academy of Sciences
Mao Xinyu
Xishuangbanna Tropical Botanical Garden, Chinese Academy of Sciences
Yu Sheng
Agricultural Genomics Institute at Shenzhen, Chinese Academy of Agricultural Sciences
Liu Guizhou
Xishuangbanna Tropical Botanical Garden, Chinese Academy of Sciences
Chengkai Lu
Wan Jinpeng
Xishuangbanna Tropical Botanical Garden, Chinese Academy of Sciences
Lingfei Hu
Zhejiang University https://orcid.org/0000-0002-7791-9440
Shaoqun Zhou
Agricultural Genomics Institute at Shenzhen
Xu Peng (xupeng@xtbg.ac.cn)
Xishuangbanna Tropical Botanical Garden, Chinese Academy of Sciences

Article

Keywords:

Posted Date: June 24th, 2022

DOI: https://doi.org/10.21203/rs.3.rs-1761850/v1

Microbiota-mediated nitrogen fixation and homeostasis in aerial root-mucilage

Zhiqiang Pang [1,2#], Xinyu Mao [1,2#], Sheng Yu [5], Guizhou Liu [1], Chengkai Lu [1], Jinpeng Wan [1], Lingfei Hu [4*], Shaoqun Zhou [5*], Peng Xu [1,2,3*]

[1] CAS Key Laboratory of Tropical Plant Resources and Sustainable Use, Xishuangbanna Tropical Botanical Garden, Chinese Academy of Sciences, Mengla, China.

[2] College of Life Sciences, University of Chinese Academy of Sciences, Beijing, China.

[3] The Innovative Academy of Seed Design, Chinese Academy of Sciences, Mengla, China.

[4] Institute of Soil and Water Resources and Environmental Science, College of Environmental and Resource Sciences, Zhejiang Provincial Key Laboratory of Agricultural Resources and Environment, Zhejiang University, Hangzhou, China.

[5] Shenzhen Branch, Guangdong Laboratory of Lingnan Modern Agriculture, Genome Analysis Laboratory of the Ministry of Agriculture and Rural Affairs, Agricultural Genomics Institute at Shenzhen, Chinese Academy of Agricultural Sciences, Shenzhen, China.

[#] These authors contributed equally: Zhiqiang Pang (pangzhiqiang@xtbg.ac.cn), Xinyu Mao (maoxinyu@xtbg.ac.cn)

[*] Corresponding author E-mail addresses: lingfeihu@zju.edu.cn (Lingfei Hu); zhoushaoqun@caas.cn (Shaoqun Zhou); xupeng@xtbg.ac.cn

Abstract

Plants sustain intimate relationships with diverse microbes. While it is well recognized that these plant-associated microbiota shape individual performance and fitness of host plants, how they exert their function and maintain their homeostasis are largely unexplored. Here, using pink lady plant (*Heterotis rotundifolia*) as a model, we investigated the phenomenon of microbiota-mediated nitrogen fixation as well as the proximal homeostasis mechanisms of this process in the aerial root mucilage. The aerial root mucilage is enriched in primary metabolites such as carbohydrates, and abundant diazotrophic bacteria. Nitrogen-labeled experiments and gene expression analysis indicate that the aerial root-mucilage microhabitat fixes atmospheric nitrogen to support plant growth. The presence of a key "police" fungus in the mucilage helps the host plant to defend against environmental microbes rather than diazotrophs. The discovery of new biological function and “police” fungi in the aerial root-mucilage microhabitat provides insights into microbial homeostasis maintenance of microenvironmental function and rhizosphere ecology.

Introduction

Plant aerial roots have distinct functions from underground roots such as anchorage, oxygen absorption

(Shekhar et al., 2019), water uptake, photosynthesis (Zotz and Winkler 2013), and support (Eskov et al., 2016, Liz Filartiga et al., 2020). Most aerial roots require to enter the soil or cling to other support to perform above function. During those process, the tip of aerial root exudes an amount of mucilage to protect root tip cells, help them enter the soil or climb up vertical surfaces of host plants (Galloway et al., 2020).

Like underground roots, the exuded mucilage on aerial root tips contains a wide array of primary and secondary metabolites, including polysaccharides, proteins, lipids, flavonoids and etc. (Galloway et al., 2020, Nazari 2021). To date, the role in nitrogen fixation mediated by mucilage of aerial roots attracts most of the attention. Recently, a promising study showed that aerial roots of Mexican maize at high nodes exude a large amount of carbohydrate-rich mucilage, which contributes 29%–82% of the plant nitrogen from atmospheric nitrogen. Analysis of mucilage microbiota indicated that it was enriched in nitrogen diazotrophic bacterial *Burkholderia*, *Herbaspirillum* and *Azospirillumin*, suggesting the mucilage-microbiota system plays an essential role in the nitrogen demand of the plant (Van Deynze et al., 2018). The carbohydrate-rich mucilage were proposed to play a key role in mediating maize-diazotrophic microbiota interactions in the aerial root, whereas the underlying mechanisms of secreting mucilage and fixing nitrogen remain unclear, the carbohydrate-rich mucilage were recognized as a hotpot zone in mediating maize-diazotrophic microbiota interactions (Bennett et al., 2020, Pang et al., 2021). In addition, the microbes inhabiting aerial root mucilage seem to always be potential nitrogen-fixing bacteria rather than pathogens or environmental microbes, such as *Burkholderia*, *Herbaspirillum*, *Pseudomonas*, *Klebsiella*, *Pantoea*, etc. (Higdon et al., 2020, Higdon et al., 2020). Those special diazotrophs have genes needed for metabolizing mucilage and carbohydrate components to fuel the energy-expensive nitrogen-fixing process, and inhabit in lowering of oxygen microenvironments (Bennett et al., 2020). Besides host plant-derived regulatory forces, the interactions among microbiota members contribute to the establishment, stability, and resilience of host-associated microbial communities (Getzke et al., 2019). For instance, the root bacterial *Variovorax* and *Pseudomonas* are able to maintain root fungal homeostasis, and promote host survive in *Arabidopsis thaliana* (Durán et al., 2018). In the second line of defense (within the root), enriched endophytic bacterial microbiota, Chitinophagaceae and Flavobacteriaceae can still become the protective layer of the host plant, functioning as a second line of defense within the root (Carrion et al., 2019). In addition, some "partner" or "police" microbes in the interaction microenvironment are also of concern, and they are friendly with the other microbes or play an important role in maintaining microbial homeostasis and defending against pathogens, such as biocontrol microbes in agriculture. A recent study showed that

soil bacteria *Paraburkholderia edwinii* as a toxin sponge to protect fungi by sequestering antibiotic phenazines (Dahlstrom and Newman 2022). Interestingly, host-microbe and microbe-microbe interactions can also simultaneously produce synergistic effects to maintain microbial homeostasis in plant roots, such as *Arabidopsis* root bacterial microbial communities and plant metabolite tryptophan jointly control soil fungal pathogens *Plectosphaerella cucumerina* to promote plant growth and health (Wolinska et al., 2021). In summary, current assumptions about plant-associated microbial homeostasis are the result of host plant-microbiota and microbiota-microbiota interactions. To find out this key "police" or "partner" mucilage compound and microbe and its protective association of diazotrophic microbiota is of great value for understanding the microbial homeostasis of mucilage-microbiota system. However, the proximal mechanisms underlying mucilage-mediated microbiota interactions as well as diazotrophic microbiota homeostasis are still largely unexplored.

Pink lady (*Heterotis rotundifolia*) is a fast-growing, perennial shrub. It is a high-risk invasive plant listed in the Global Compendium of Weeds (PIER 2013, Randall 2012). Their aerial roots vary from 0.1 cm to 16 cm and exude a large amount of mucilage before reaching the ground (Fig. 1a). Efficient uptake and utilization of nitrogen by plants seems to contribute to their successful invasion, a process that is accompanied by early reproduction and many offspring and high growth rates (Feng et al., 2009, Funk and Vitousek 2007). Given that the roles of aerial roots in nitrogen uptake stated above, the aerial root-mucilage-microbiota system may contribute to its rapid nitrogen-fixing to achieve their rapid growth and spread. In this study, we use this easy-to-cultivate small plant as a model to answer the following two scientific questions: what is the biological function of the aerial root-mucilage microhabitat and underlying mechanisms? As a "natural medium", how does mucilage maintain its function and internal microbial homeostasis?

Results

Aerial root mucilage and underground root exudate of *H. rotundifolia* have distinct biochemical composition

The creeping *H. rotundifolia* plants can grow over 2 meters long and form a single aerial root at each stem node (Fig. 1a). These mucilage-producing aerial roots vary from barely visible to naked-eyes to over 14 cm in length. We compared the biochemical composition of the Aerial Root Mucilage (ARM) and Underground Root Exudates (URE) by collecting widely-targeted metabolomics data of these samples (Fig.

1b) (Chen et al., 2013). Principal-component analysis (PCA) result demonstrated a clear differentiation of metabolic profile of ARM and URE samples (Fig. 1c). Indeed, 531 of the 1,033 putatively annotated metabolites were significantly different between these two samples (P < 0.01, Table. S1 and Fig. S1). Whereas URE tended to contain higher levels of lipids and alkaloids (Secondary metabolites are major components), ARM was found richer in amino acid derivatives, nucleotide derivatives, flavonoids and carbohydrates (primary metabolites are the main components, Fig. 1d). This is consistent with the more viscous nature of ARM. Further carbohydrate measurement with a targeted approach confirmed that the ARM was rich in glucose, fructose and sucrose, which were barely detectable in URE (< 0.01mg·g^{-1}; Fig. 1e).

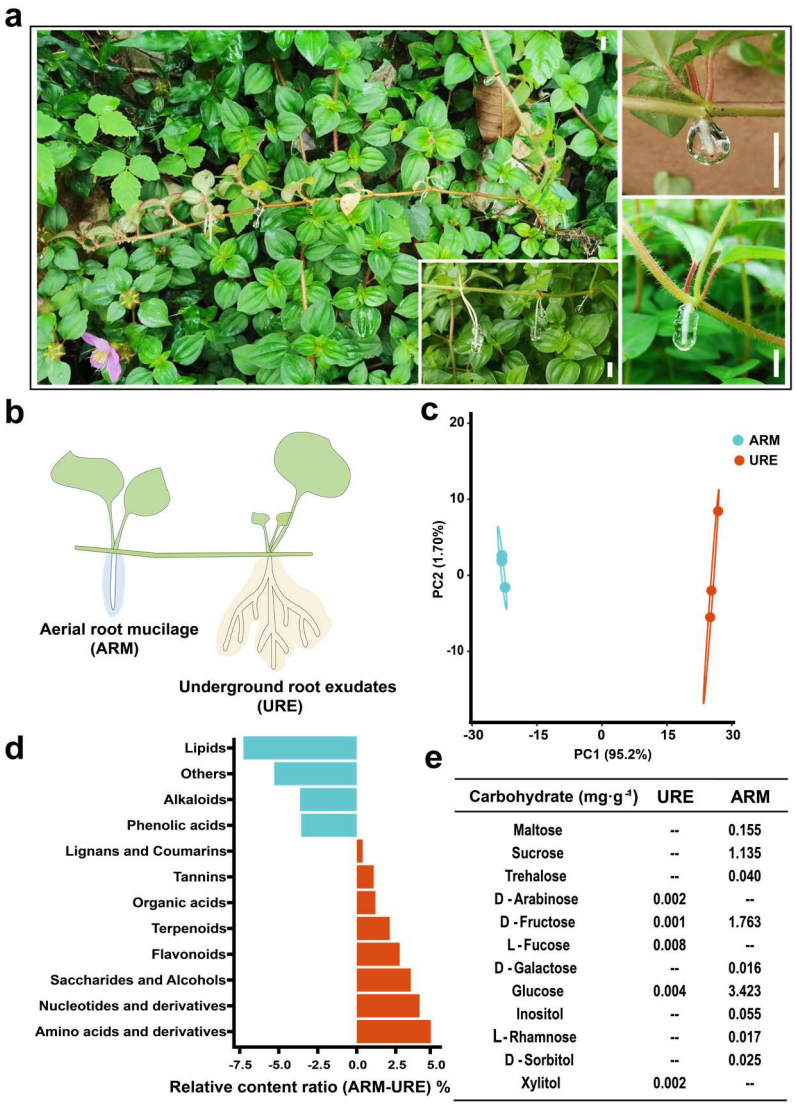

Carbohydrate (mg·g^{-1})	URE	ARM
Maltose	--	0.155
Sucrose	--	1.135
Trehalose	--	0.040
D-Arabinose	0.002	--
D-Fructose	0.001	1.763
L-Fucose	0.008	--
D-Galactose	--	0.016
Glucose	0.004	3.423
Inositol	--	0.055
L-Rhamnose	--	0.017
D-Sorbitol	--	0.025
Xylitol	0.002	--

Fig. 1 Aerial root mucilage (ARM) and underground root exudate (URE) compound of *H. rotundifolia*. a, Creeping *H. rotundifolia* with aerial root and mucilage of varying lengths. White scale bars =1 cm. **b**, Sampling diagram of aerial root mucilage and underground root exudates. **c**, Principal component analysis result of widely-targeted metabolome of ARM and URE. **d**, Relative content of different compounds of ARM and URE.

Blue indicates that those content of URE is higher than that of ARM, and red indicates that the content of ARM is higher than that of URE. **e**, Carbohydrate content of aerial root mucilage and underground root exudate, on average, n = 6.

Aerial root mucilage microbiota of *H. rotundifolia* is enriched in diazotrophic bacteria

As underscored by their biochemical differences, ARM and URE likely represent distinct ecological niches that are suitable to host different microbiota. To test this hypothesis, we collected aerial root mucilage, rhizospheric samples and environmental soil at five separated sites in Xishuangbanna Tropical Botanical Garden (Xishuangbanna, China), and examined their prokaryotic and eukaryotic microbiota through 16S rRNA and ITS gene sequencing (Table. S2 and Fig. S2). In support of our hypothesis, unconstrained principal coordinate analysis (PCoA) analysis based on the Bray–Curtis metric revealed that both the bacterial and fungal composition of ARM were distinct from those of rhizospheric and bulk soil, which were similar to each other (Fig. 2a bacteria and S2a fungi). Notably, the prokaryotic taxonomic diversity of ARM was lower than rhizospheric and bulk soil, indicative of a specialized bacterial community in ARM (Fig. 2b). For fungal communities, there was no significant difference in alpha diversity among the three ecological niches (Fig. S2b). A total of 233 differentially enriched bacterial genera and 65 fungal genera were identified between ARM and rhizosphere soil (Wilcoxon rank-sum test, $P < 0.05$, Table. S3). Specifically, ARM contained higher load of *Burkholderia*, *Herbaspirllum* and *Novosphingobium*, whereas the relative abundance of *Bacillus*, *Gaiella* and *Nocardioides* were higher in underground samples (Fig. 2c and S3a-d).

The top two ARM-enriched bacterial genera, *Burkholderia* and *Herbaspirllum* include numerous diazotrophic species that have been widely used as model systems of plant-associated nitrogen-fixing microbes (Bloch et al., 2020). Unfortunately, we were not able to produce any single-strain culture in these genera under all accessible culturing conditions including anaerobic incubation (Table. S4 and Fig. S4a). Some of the single-strain culture we obtained that were identified as *Klebsiella*, *Sphingobacterium*, *Cupriavidus*, *Acinetobacter* and *Pantoea* species were able to grow on nitrogen-free medium. From these species, we were able to clone different alleles of the key nitrogen fixation gene, *nif*H (Table. S4). In addition, bacterial function annotation showed that aerial mucilage has a higher nitrogen fixation capacity than rhizosphere soil (Wilcoxon rank-sum test, $P<0.05$, Fig. S3e, f). A number of these species further demonstrated nitrogen fixation activity in $^{15}N_2$-labeled experiments (Fig. S4b). These data lead us to hypothesize that nitrogen fixation is a key function of the bacterial community associated with *H.*

rotundifolia ARM.

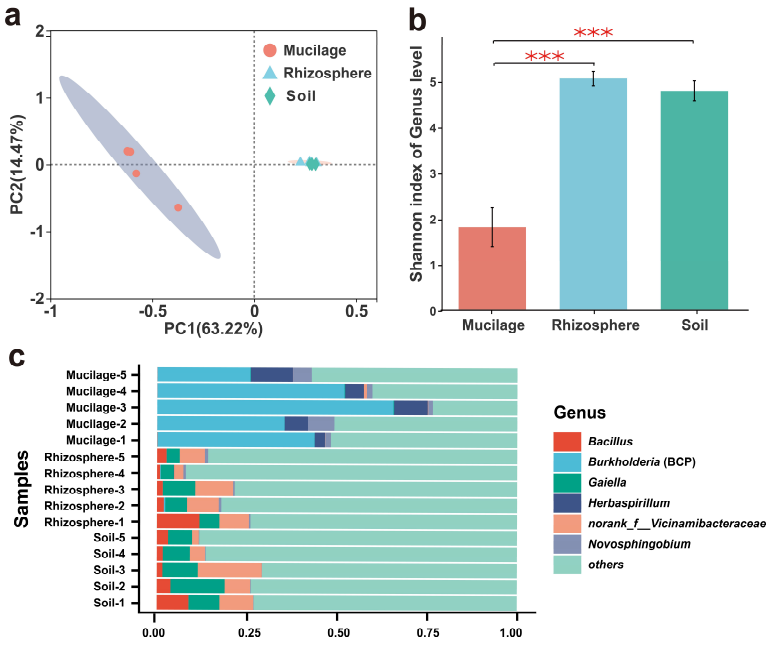

Fig. 2 Bacteria diversity and community of aerial root mucilage (mucilage) and underground rhizosphere soil (rhizosphere). **a**, Unconstrained PCoA with Bray–Curtis distance showing that the bacteria of mucilage separate from those of rhizosphere and soil in the first axis ($P < 0.001$, permutational multivariate analysis of variance (PERMANOVA) by Adonis). **b**, Shannon index of the bacteria of aerial root mucilage, underground rhizosphere soil and the corresponding bulk soils. **c**, Genus-level distribution of bacterial communities in mucilage and rhizosphere soil. *Burkholderia*, *Herbaspirllum*, *Novosphingobium* are higher relative abundance in mucilage (59.09%, 10.43% and 5.36%, respectively) than in underground rhizosphere soil (0.14%, 0.22% and 0.64%, respectively). The numbers of replicated samples in this figure are as follows: mucilage (n = 5), rhizosphere soil (n = 5), soil (n = 5).

Aerial root mucilage of *H. rotundifolia* fixes atmospheric nitrogen to support plant growth

To test if nitrogen fixation could occur in intact ARM microbiota, we performed ^{15}N labeled nitrogen gas ($^{15}N_2$) feeding experiments with segments of *H. rotundifolia* stems with mucilage-bearing aerial roots, aerial roots with mucilage artificially-removed, or aerial roots removed as a whole (Fig. 3a). When fed with 20% $^{15}N_2$, plants with mucilage-bearing aerial roots contained significantly higher relative abundance of ^{15}N in all tissues measured compared to those with aerial roots only or no aerial roots at all (Fig. 3b-e and Table. S5). This supports our hypothesis that intact ARM microbiota can facilitate incorporation of atmospheric nitrogen. To further test whether this, ARM-dependent nitrogen fixation is ecologically relevant for the fitness of *H. rotundifolia* in greenhouse, we compared the growth of plants with aerial roots artificially

removed versus sympatric no operation controls in a field experiment. Four months after our operations, plants with aerial roots weighed 10% heavier in dry mass compared to those without, suggesting that the aerial roots, along with the microbiota hosted in their associated mucilage, can play non-trivial roles in supporting the growth of *H. rotundifolia in situ* (Fig. 3f and Table. S5).

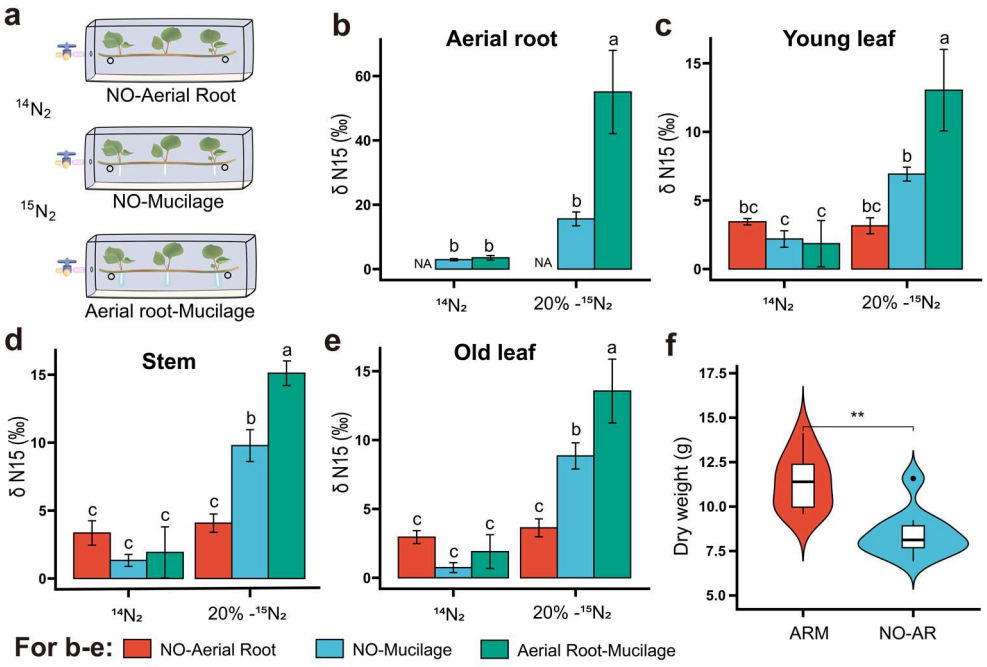

Fig. 3 Aerial root-mucilage is the main site for nitrogen fixation in *H. rotundifolia* aerial root. a, Illustration of the incubation set-up enabling the study of the transfer of aerial mucilage fixed (^{15}N-enriched) N_2 from the air to the plant. The plant types include no aerial root plant (NO-Aerial Root), aerial root plant without mucilage +(NO-Mucilage), and aerial root plant with mucilage (Aerial Root-Mucilage). **b-e**, Analysis of different *H. rotundifolia* samples for $^{15}N_2$ enrichment in aerial root (e), young (d) and old leaf (f), and stem (e). Box plots show combined data from six independent experiments with natural nitrogen or replace 20% (V) of nitrogen with $^{15}N_2$ for 72 h. $^{14}N_2$ and no aerial root plant (NO-Aerial Root) samples were used as negative control groups. Different letters indicate significantly different groups ($P < 0.05$, Two-way ANOVA, n = 3). **f**, The dry weight of plant aboveground was significantly reduced after removal of aerial root (NO-AR, $P < 0.01$, T-Test, n = 10). The fresh weight of aerial root tissues removed were less than 10 milligrams per plant.

Tissue-specific gene expression in mucilage-secreting aerial roots could facilitate efficient carbon-nitrogen exchange with mucilage microbiota

Nitrogen fixation is a complex symbiotic relationship that requires extensive collaboration between the host plants and the diazotrophes at molecular level. To investigate the molecular interaction between *H. rotundifolia* and its ARM microbiota, we sequenced the *H. rotundifolia* genome with a combination of 61.86 G PacBio CLR reads and 20.1 G Hi-C reads to obtain a chromosome-scale reference genome assembly, which was subsequently used to map short-read RNAseq data for transcriptome-wide gene expression

profiling. The reference assembly we obtained was estimated to be 171.44 Mb, similar to a previous estimation (180 M, Fig. S4). The contig N50 length was 8.39 Mb and the scaffold N50 length was 11.23 Mb (Fig. 4a; Table 1). In this assembly, we annotated 29,574 putative gene models and 2,434 noncoding RNAs, and the assembly was estimated to be 98% complete through Benchmarking Universal Single-Copy Ortholog analysis (Table 1 and S5). Over 96% of the predicted genes were functionally annotated through gene ontology (GO), Kyoto Encyclopedia of Genes and Genomes (KEGG), Swissprot, TrEMBL, and Pfam databases (Table. S6).

Table 1. Assembly and annotation of the genome of the *H. rotundifolia*

Survey	
Sequencing platform	PacBio Sequel II
K-mer	17.00
K-mer Depth	85.00
Heterozygous ratio (%)	0.57
Estimated genome size (Mb)	192.57
Assembly	
Assembly size (Mbp)	171.44
Contigs N50 (Mb)	8.39
Scaffold N50(Mb)	11.23
GC content (%)	43.88
Contig number	39.00
Contig length proportion	99.28
Annotation	
Total gene	29,572
Annotated gene	28,583
Total TE (%)	22.31
LTR (%)	15.78
Non-protein-coding genes	2434
miRNA	97
tRNA	492
rRNA	1731
snRNA	114
BUSCO completeness (%)	98.00

We then obtained RNA-seq data from aerial roots with or without mucilage and underground roots to identify transcriptome-wide gene expression differences in these tissues (Fig. 4b). Functional enrichment analyses results based on GO and KEGG annotations revealed that genes related to photosynthesis and phenylpropanoid metabolism were preferentially expressed in aerial roots, and these differences in gene expression were more pronounced when comparing mucilage-bearing aerial roots and underground roots (Table. S7; Fig. 4c-d). Stable plant-diazotrophe symbiosis is built upon extensive carbon flow from the host plant to the microbes, accompanied by nitrogen flow in reverse (Bennett et al., 2020, Yang et al., 2022).

Hence, we specifically examined the expression of carbohydrate and accessible nitrogen transporter genes in the three tissues. In result, expression of both putative sugar transporters (*e.g. STP, SWEET, INV*) and nitrate/nitrite transporters and assimilation genes (*e.g. AMT*, *NRT* and *GS*) were significantly higher in mucilage-bearing aerial roots than those without mucilage, indicative of more active carbon-nitrogen flow when the mucilage is present (Fig. 4e). Interestingly, the putative nitrate and nitrite transporters highly expressed in mucilage-bearing aerial roots were also highly expressed in underground roots (with the notable exception of *NRT2.1*), whereas the putative carbohydrate transporter were expressed at higher levels in mucilage-bearing aerial roots than underground root.

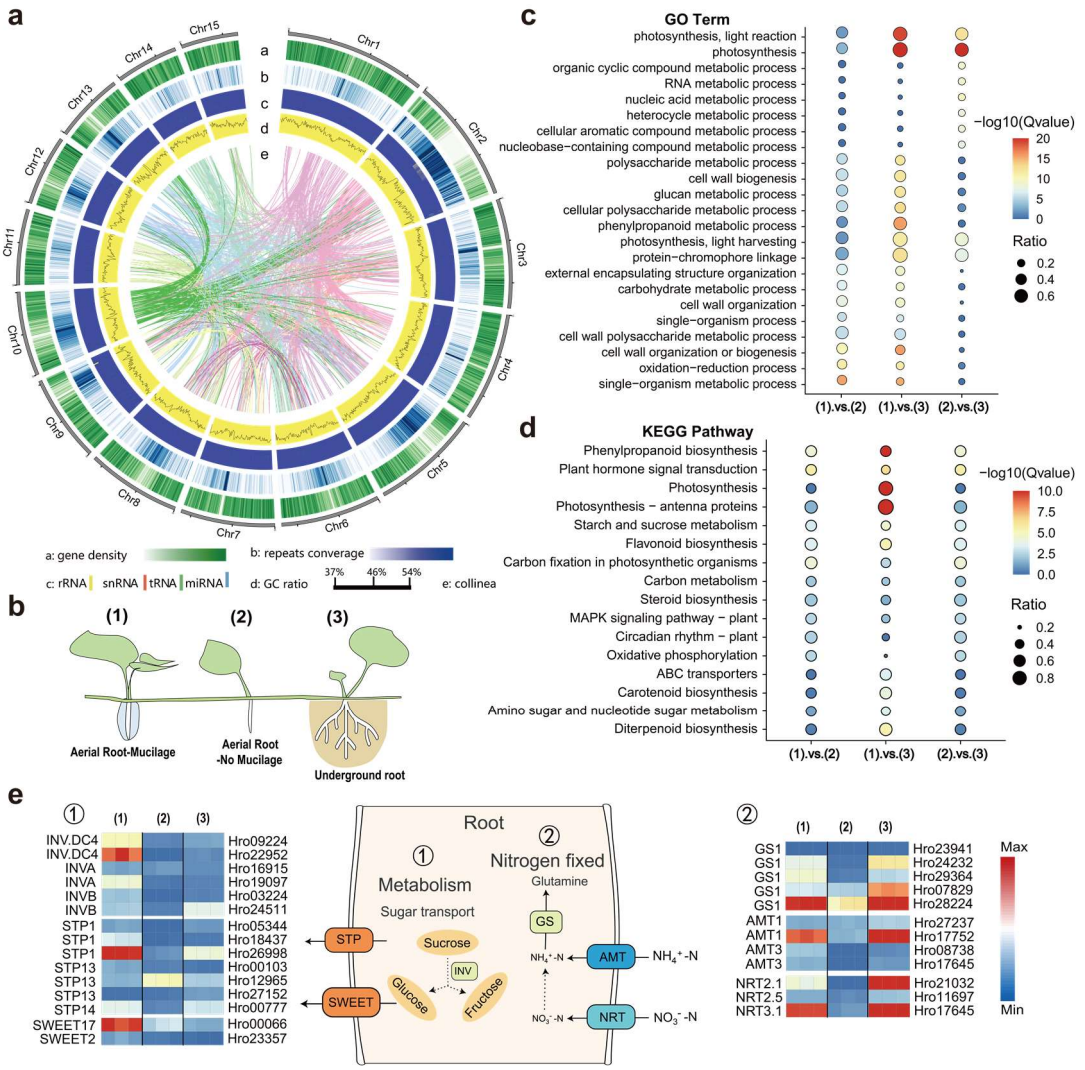

Fig. 4 Genomic characterization and transcriptome of *H. rotundifolia* reveal biological function of aerial root-mucilage. a, Genomic landscape of the 15 assembled *H. rotundifolia* chromosomes. **b**, Overview of samples aerial root-mucilage and no mucilage, and underground root of *H. rotundifolia*. (1): Aerial roots with mucilage; (2): Aerial roots without mucilage; (3): Underground root sample without mucilage. **c-d,** Go (c) and KEGG (d) enrichment pathway of mucilage and no mucilage aerial root. The selected each sample top 10 categories are shown. **e**. Expression patterns of nitrogen fixed and plant metabolism genes in the different root

and types. ① and ② are overview of pathways of nitrogen utilization and sugar transport. Genes with expression FPKM < 10 were not visualized in the heatmaps.

Mucilage-dwelling *Chaetomella raphigera* selectively inhibit environmental but not sympatric microbes

Though the carbohydrate-rich ARM of *H. rotundifolia* creates an ideal niche for diazotrophic bacteria, it is also potentially prone to disturbance by environmental microbes that are commensal or even pathogenic to host plants. Though there is a rich literature on the microbiota structuring function of exuded plant specialized metabolites, we were not able to identify any specific compound that displayed obvious antibiotic function when screening the twenty most abundant metabolites in the ARM at physiologically relevant concentration (Fig. S6 and Table S10-11).

The alternative explanation for the homeostatic diazotrophic microbiota is that certain members of the community could selectively allow the growth of the diazotrophes, but inhibiting unwelcomed environmental microbes. To identify potential “police” microbes in the ARM microbiota, we collected 16 single-spore/single-colony isolates from bulk ARM samples, and screened their broad-spectrum antibiotic activity by culturing on rich media exposed to open air. Through this screening, one fungal culture F-XTBG8 remained uncontaminated after 5 days of exposure to airborne microbes, and was identified as *Chaetomella raphigera* by ITS sequencing (Fig. 5a, S7 and Table. S8). Subsequent *in vitro* antibiotic tests demonstrated that this isolate of *C. raphigera* could inhibit the growth of over 100 common phytopathogens and environmental fungi including *Fusarium oxysporum, F. solani,* and *Magnaporthe oryzae* (Fig. 5a-b and S7). Interestingly, liquid culture of this *C. raphigera* strain demonstrated clear inhibitory effect against aerial and soil bacterial communities *in vitro,* but this effect significantly diminished when tested against rhizopheric bacteria of *H. rotundifolia*, and was completely abolished when tested against ARM bacteria (Fig. 5c). Consistently, liquid culture of *C. raphigera* suppressed the growth of a generic bacteria *Escherichia coli* DH-5a *in vitro*, but showed no inhibitory effect against any of the six bacterial strains isolated from *H. rotundifolia* ARM (Fig. 5d).

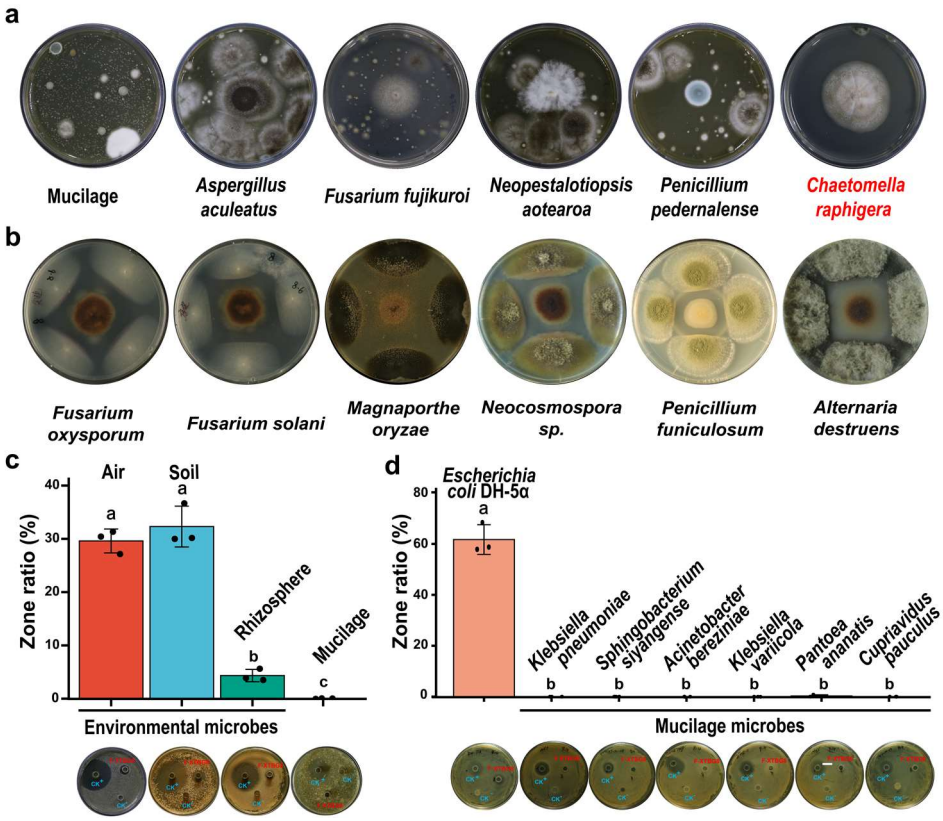

Fig. 5 A "police" fungi of mucilage and nitrogen fixing bacteria. a-b, Interactions between different microbes and environmental fungi. Only *C. raphigera* (F-XTBG8) shows the resistance to the plant pathogenic fungi and various fungi from environment (**b**). **c-d**, F-XTBG8 fungal metabolites are resistant to air and soil environmental bacteria (and DH-5α), but not to nitrogen-fixing bacteria of mucilage. The zone ratio is equal to the zone of inhibition of the culture of F-XTBG8 divided by the positive control (antibiotic streptomycin and tetracycline hydrochloride).

Discussion

Aerial roots are known to facilitate gas exchange in submergence-tolerant plants, provide additional mechanic support for climbing vines, or function as the primary site of nutrient uptake in marginal habitats (Shekhar et al., 2019). Mucilage has been proposed to maintain a moisturized interface and provide lubrication and protection for aerial roots (Nazari 2021). Microbiome studies in the last decade have revealed significant functions for the diverse microbial communities associated with plant rhizosphere, and have inspired similar investigation into the biochemical and microbial diversity in ARM (Amicucci et al., 2019, Bennett et al., 2020, Higdon et al., 2020, Higdon et al., 2020, Pozzo et al., 2018). In a mucilage-secreting tropical maize landrace, microbes isolated from the carbohydrate-rich mucilage have been demonstrated to fix atmospheric nitrogen to promote plant growth (Van Deynze et al., 2018).

In this study on *H. rotundifolia,* we confirmed that ARM and URE had distinct biochemical composition from each other, both in terms of primary and specialized metabolites (Fig. 1). This biochemical differentiation correlated with the distinctive prokaryotic communities associated with aerial and underground roots (Fig. 2). Since the environmental microbial composition has a strong impact on the structure of plant-associated microbiota, the inherently different airborne and soilborne microbial communities is likely a predominant factor in deciding the microbial diversity in ARM and URE. Yet, the biochemical differences between ARM and URE likely play a role in structuring their associated microbiota as well. From the nutritional perspective, ARM was rich in amino acids, nucleotides, and carbohydrates, which provided a different niche from the lipid-rich URE (Fig. 1d) (Koprivova and Kopriva 2022, Macabuhay et al., 2021, Pang et al., 2021, Sasse et al., 2018). Furthermore, the terpenoid- and flavonoid-rich ARM could impose a distinct selective pressure on microbes compared to URE, which contained higher levels of alkaloids and phenolic acids (Fig. 1d).

Comparison of microbial community composition between URE and ARM revealed that a number of known diazotrophic bacterial genera were enriched in the ARM (Fig. 2c). In our study, based on bacterial function prediction and nitrogen labeled experiment, we can conclude that the aerial root-mucilage microhabitat harbors diazotrophic microbiota such as diazotrophs *Klebsiella, Pantoea*, *Sphingobacterium*, *Herbaspirillum* and *Burkholderia*. These bacteria are widely used model systems to study the associative nitrogen-fixing, and already well utilized for agricultural production (Bloch et al., 2020, Eke et al., 2019, Higdon et al., 2020, Pankievicz et al., 2015, Pankievicz et al., 2019). Consistently, subsequent stable isotope tracking experiment showed that atmospheric nitrogen could be incorporated into plant biomass in an aerial root and mucilage dependent manner (Fig. 3a-e). We further demonstrated that removal of aerial roots could significantly impact plant biomass in a four-month-long field experiment (Fig. 3f). This result could partially support of ecological relevance of ARM-mediated nitrogen fixation for plant fitness *in situ*, though we also recognize that the operation of aerial root removal could have complex influence on plant growth that may not be dependent on the mucilage microbiota. Although the aerial root-mucilage-diazotrophic microbiota system was able to fix nitrogen, we expect to inoculate single bacteria or microbial communities for further discovery of core nitrogen-fixing bacteria and genes. In addition, aerial roots without mucilage also showed a nitrogen fixation ability to some extent, which may be caused by the incompletely removed mucilage or endogenous nitrogen-fixing bacteria in aerial roots.

Since nitrogen fixation involves dynamic nitrogen-carbon exchange between the symbiotic partners, we

hypothesized that the aerial roots of *H. rotundifolia* to be highly active in nitrogen and carbon transportation. To test this hypothesis, we generated a chromosome-scale genome assembly of *H. rotundifolia* with PacBio CLR and Hi-C technologies and RNA sequencing data, which was then used for comparative transcriptomics analyses (Fig. 4). In support of our hypothesis, a number of sugar transporters were exclusively expressed in mucilage-bearing aerial roots when compared to aerial roots with no mucilage and underground roots (Fig. 4e). Interestingly, three of the five nitrogenous compound transporters highly expressed in underground roots were also expressed in aerial roots in a mucilage-dependent fashion (Fig. 4e) (Liu et al., 2022). This expression pattern strongly suggests that the present of ARM could induce the expression of nitrogenous compound transporters. This is consistent with previous observations in seagrass. The nitrogen-fixing symbionts live within the seagrass root tissue, where it supplies amino acids and ammonia to the host in exchange for sugars (Mohr et al., 2021).

The plant innate immune systems and special metabolites play important roles in shaping the host-associated microbiota (Castrillo et al., 2017, Chen et al., 2020, Lebeis et al., 2015). Recently research found that the host plant factors shape the plant-association microbiota community, those secrete signals to recruit specific microbiota while generating molecules that are toxic to others (Macabuhay et al., 2021, Thoms et al., 2021). Such as, plant special metabolites triterpenes, coumarin, flavonoid and benzoxazinoid are key compounds modulating plant microbiota composition (Cadot et al., 2021, Cotton et al., 2019, Harbort et al., 2020, Hu et al., 2018, Kudjordjie et al., 2019, Pang et al., 2021, Schütz et al., 2019), and root secretes coumarin to against pathogens and impact the assembly of rhizosphere microbiota (Stringlis et al., 2018). Moreover, the important of plant metabolites or root exudates in defense pathogens and maintain microbial homeostasis in the rhizosphere is increasingly recognized, such as volatile organic compounds, tryptophan, phytohormones and camalexin (Hammerbacher et al., 2019, Koprivova et al., 2019, Macabuhay et al., 2021, Pang et al., 2021, Sharifi et al., 2018, Stassen et al., 2020, Wolinska et al., 2021). It is reasonable to speculate that the specialized compounds of aerial root mucilage to recruit special microbiota as nutrients, but also some proteins and compounds that could serve as antibiotics to defense pathogenic and environmental microbe or maintain the homeostasis of the mucilage-microbiota system. A hint at answer the question may be found in our potential mucilage and other compounds (Table S10): gallic acid, epigallocatechin gallate, phthalic anhydride and others have a certain inhibitory effect on pathogens, but these compounds are low concentrations in mucilage and the relationship between metabolites and microbial homeostasis needs to be further explored. Whether plant special metabolites

play an important regulatory role in the aerial root-mucilage microenvironment should further consider and expand list of candidate metabolites. In addition, preeminent research has shown that maize root secretes flavones that attract the enrichment of the rhizosphere bacterial taxa Oxalobacteriaceae, thereby nitrogen acquisition and promoting growth in nitrogen-poor soils (Yu et al., 2021). This has some inspiration for our research, we also found that aerial root mucilage has a higher content of flavonoids. It is still unknown how and which metabolites are recruitment for shaping functional diazotrophic microbiota in the aerial root mucilage of *Heterotis rotundifolia* and worth further study with plant transcriptome (and metatranscriptomics), metabonomic and metagenomics. In addition, we found that mucilage production always follows the high humidity in the environment (Table. S9), and future studies should reveal the causality between the dynamic basis of mucilage exudates and environment factors.

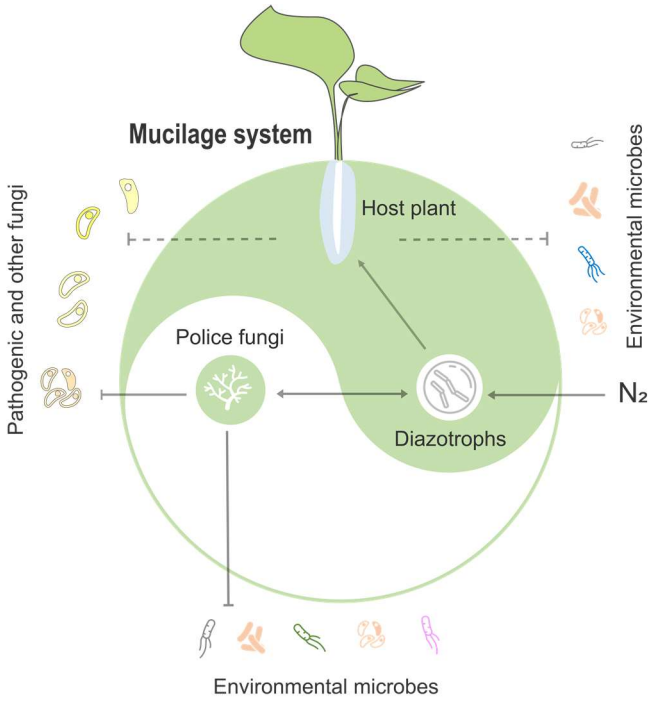

Fig. 6 The model of aerial root-mucilage-microbiota system. The friendly relationship between "police" fungi and diazotrophic microbiota in the aerial root-mucilage microhabitat. The "police" fungi have a broad spectrum of resistance to environmental and pathogenic microbes rather than functional bacteria. The aerial root-mucilage may screen and resist microbes of environment.

The current hypothesis is that microbial homeostasis in plant roots is main maintain by both microbiota-microbiota and host plant-microbiota and interactions, whereas little is known of those distinct outputs in maintaining microbial homeostatic between the plant and its root microbiota (Getzke et al., 2019, Wolinska et al., 2021). Our discovery of *Chaetomella raphigera* (F-XTBG8)-the ‘‘police’’ fungi that helps mucilage

and diazotrophic bacteria withstand pathogenic and environmental microbes-establishes that the existence of such beneficial partnerships in aerial root-mucilage microhabitat. Previous study showed that the root microbiota homeostasis has an important regulatory role in nitrogen-fixing symbionts and the adaptation of plants to different environment. For instance, the rhizosphere microbiota *Bacillaceae* group promotes the nodulation of rhizobia *Sinorhizobium* and soybean growth under saline-alkali conditions under saline–alkali conditions (Han et al., 2020). Likewise, a recent study found that the facultative biotrophic fungus *Phomopsis liquidambaris* facilitates the migration of rhizobia from the soil to the peanut rhizosphere, thus triggering peanut-rhizobia nodulation (Zhang et al., 2020). Those relationships may be common in plant-microbiota interactions, and interesting findings may have fundamental practical implications (Dahlstrom and Newman 2022). Moreover, F-XTBG8 was not only nutritionally competitive with other environmental and pathogenic microbes, but its metabolites had inhibitory effects on those microbes and not inhibitory on diazotrophic bacteria in the mucilage. Further study could related to microbial cross-feeding of “police” and functional microbes, which refers to interactions between microbes in which molecules metabolized by one microbe are further utilized by another microbe (Smith et al., 2019). Extensive cultivation of these nitrogen-fixing microbes and further exploration of the molecular basis for the friendly coexistence of these microbes with "police" fungi from the genes, transporters and metabolic gene clusters are necessary. Our study emphasis on the key role of the “police microbe” controlled aerial root-mucilage-diazotrophic microbiota microenvironment and the biochemical conversation that dominate it. Further investigation of the fungal metabolites and broad-spectrum antimicrobe mechanisms of "police" fungi will help us to decipher the specific interaction of mucilage-microbiota and the underlying mechanism of microbial homeostasis. The predicted results of the metabolic genes of terpenoids and polyketides in its genome will help us to further target potential antibacterial compounds (unpublished data). Moreover, the origin of this fungus and diazotrophic bacteria needs to be further determined which may be from plant-borne ("vertical transmission") or environment are unresolved. Collectively, our concepts provide a study paradigm for understanding how plant may engage with functional microbiota while restricting pathogens and environmental microbes.

Our study found a novel role for aerial root-mucilage microhabitat in nitrogen uptake, and extended the concept of rhizosphere, that aerial roots can still perform the same biological functions as underground roots. More importantly, the discovery of "police" fungi in mucilage further advances our understanding of the homeostasis mechanisms of specific functional microbiota in microenvironment (Fig. 6). This further

confirms that plants actively mediate plant-microbiota interactions and maintain microbial homeostasis and could have an important impact on nitrogen use efficiency, rapid growth, and invasion of *H. rotundifolia*. The "police" microbe insight has important understanding for diverse problems concerning plant microbiota assembly and environmental microbes. We hope that the aerial root-mucilage-functional microbiota system established in this study will enable basic biological insights to be gained for biological interactions.

Methods

Plant samples

H. rotundifolia maintained by Xishuangbanna Tropical Botanical Garden (Xishuangbanna, China) was sampled between June 2019 and December 2021. Collectively, these concepts provide a paradigm for understanding how plants may engage with beneficial microbes while restricting pathogens.

Metabolite profiling.

Aerial root mucilage and underground root exudate collection

In May 2020, we choose three creeping *H. rotundifolia* plant that different growth stage and sampled aerial root mucilage and underground root exudate. Use sterile forceps to load the aerial root mucilage into a 50 mL centrifuge tube. For underground root exudate collection, roots were repeatedly washed and shook in 200 mL deionized water and collected promptly after root washing for 2 h by 60 rpm. All mucilage and exudate samples were immediately frozen to −80°C and then freeze-dried (MM400, Retsch) for 1.5 min at 30 Hz. Take 40 mL of the sample after mixing, place 50 mL of the centrifuge tube, and then immerse the sample in liquid nitrogen as a whole. Powder (100 mg) was weighed and extracted overnight at 4°C with 1 mL 70% methanol, followed by centrifugation for 10 min at 12 000 g. The supernatants were collected separately and combined, followed by filtration 0.22 mm pore size. For metabolome analysis, mucilage and exudate samples were analyzed using an ultrahigh-performance liquid chromatography (SHIMADZU Nexera X2)-tandem mass spectroscopy (Applied Biosystems 4500 QTRAP) (UPLC-MS/MS) based widely targeted metabolome method by Wuhan Metware Biotechnology Co., Ltd. (Wuhan, China) (http://www.metware.cn/). Carbohydrate contents were detected based on an Agilent 7890B gas chromatograph coupled to a 7000D mass spectrometer (GC-MS) platform by Metware. Concentration determination of candidate compounds (gallic acid, epigallocatechin gallate, phthalic anhydride and others) in mucilage using high-performance liquid chromatography and ultra-performance liquid chromatography-

mass spectrometry (Supplementary Methods 1 for details regarding the protocol).

Mucilage and soil DNA extraction, 16S rRNA and ITS gene sequencing

In our study, the rhizosphere soil was defined and collected as previous reported (Van Deynze et al., 2018). Aerial root mucilage and underground rhizosphere soil and bulk soil sample DNA were extracted using the FastDNA SPIN Kit for Soil (MP Biomedicals, USA) according to the manufacturer's protocol. The fungal ITS1 region (ITS1F/ITS2R) (Adams et al., 2013) and the bacterial 16S rRNA gene (V3-V4, 338F/806R) (Huse et al., 2008) were amplified. Amplicon libraries were sequenced on the Illumina MiSeq PE300 platform by the Majorbio Bio-Pharm Technology Co., Ltd. (Shanghai, China).

The 16S rRNA and ITS gene sequencing reads were demultiplexed by Fastp (version 0.20.0) (Chen et al., 2018) and merged with FLASH (version 1.2.7) (Magoč and Salzberg 2011) following: Operational taxonomic units (OTUs) with 97% similarity were clustered using UPARSE (version 7.1) (Edgar 2013). Taxonomic assignment was performed using the bacterial SILVA reference database (v12_8,) and fungal UNITE database (v7.0). Functional prediction (Tax4Fun, PICRUst1/2, BugBase phenotype prediction) was analyzed on the free online platform of the Majorbio Cloud Platform (www.majorbio.com).

Bacteria and fungi isolation in mucilage and rhizosphere

Fungi isolated from the mucilage and rhizosphere were placed onto potato dextrose agar (PDA, Hopebio, Qingdao) and incubated for 7 days (in the dark at 28°C). Five grams of rhizosphere was weighed into a 50 ml centrifuge tube, and 100 µl of 10^{-3} and 10^{-4} diluents was soaked up with diluted spreading onto tryptic soy agar (TSA, Hopebio, Qingdao), LB agar, and nitrogen-free agar (Ashby, Rhizobium, Associations and Nitrogen-free Culture-medium, Hopebio, Qingdao) to isolate diazotrophic bacteria. For bacterial culture in mucilage, 100 uL was spread directly on the above culture medium. Pure culture isolates were obtained by the streak plate or single-spore technique. ITS and 16S rRNA genes of the isolated strains were amplified with fungal primers ITS1F (5′-CTTGGTCATTTAGAGGAAGTAA-3′) and ITS4R (5′-TCCTCCGCTTATTGATATGC-3′) and bacterial universal 27F (5′-GAGAGTTTGATCCTGGCTCAG-3′) and 1492R (5′-ACGGATACCTTGTTACGACT-3′). ITS and 16S sequences were aligned with the NCBI ITS (Fungi) and 16S rRNA sequences (Bacteria) databases by Nucleotide BLAST (https://blast.ncbi.nlm.nih.gov/Blast.cgi) to determine the approximate phylogenetic affiliation. The core nitrogen fixation genes (*nif*) from known diazotrophs and maize mucilage microbiota as previously published (Dos Santos et al., 2012, Van Deynze et al., 2018) as a reference.

$^{15}N_2$ gas-enrichment experiments and analysis

The three types of no-aerial root, no-mucilage, and have aerial root-mucilage plants (None of them have underground roots, about 18 cm length) were collected from healthy *H. rotundifolia* plant. For Isotope ratio mass spectrometry (IRMS) study, we construct a experimental device for $^{15}N_2$-labelling experiments, a clear 565 mL plastic bottle, equipped with an intake valve and a device for fixing plants (Fig. 3a). After simply washing the sampled plants material with sterile water, place sterile filter paper on the bottom layer of bottle and add 2 mL sterile water for moisturizing. Then, the 0% (negative controls), 5%, 10% and 20% (v/v) of $^{15}N_2$ gas (99.9% purity, Wuhan Isotope Technology, Co., Ltd, Wuhan, China) was pumped into the bottle, and the samples were moved to phytotron at 25°C for 72 h (and some of 48 h).

For the nitrogen-fixation bacteria strain, the bacteria liquid of logarithmic growth stage (2 weeks of age) was added into 125 mL conical flask, sealed and replaced with 99.9% $^{15}N_2$ by 10% of the volume of gas in the flask with a syringe. Culture was continued at 28°C for 24 h, and strain cells were collected through Whatman glass microfiber filter (GF/F, GE Healthcare). After drying, grinding and weighing, the ^{15}N of individual aerial root, young and old leaf, stem from each plant and bacterial strains were measured using EA-HT elemental analyzer (Thermo Fisher Scientific, Inc., Bremen, Germany) coupled to an isotope ratio mass spectrometer (DELTA V Advantage, Thermo Finnigan). The isotopic composition analysis was performed at Tsinghua university Stable Isotope Facility (Shenzhen, China) and Central laboratory of Xishuangbanna Tropical Botanical Garden (Xishuangbanna, China).

Microbial antagonism experiment

To identify mucilage compounds and microbes with broad-spectrum resistance, the compound and isolates were purified and transferred to new medium plate for 24 h in advance (bacteria 12 h), and then placed outdoors (exposed to airborne microbial infection) 5 days with the cover of the petri plate open. Medium plate that does not grow other microbes were considered to have broad spectrum resistance. The efficacy of fungi strain ‘F-XTBG8’ was tested against environment and pathogenic fungi on potato dextrose agar (PDA) medium plates. Fungal culture plate agar discs (6 mm) of environment and pathogenic fungi were disposed in all around at the center of F-XTBG8 strain in a square at 1.8 cm distance, and incubated at 30°C until mycelial growth had fill medium plates. The Oxford cup method was used for the fungal metabolite and bacteria antagonism experiment. (the cup height of 10 mm, inner diameter of 6 mm, outer diameter of 8 mm). Then, 100 uL of each bacterial suspension (OD_{600}=1) were spread evenly on TSA plates, while three sterilized Oxford cups were placed in each TSA plate, and three cup were inoculated separately with 200 uL of antibacterial streptomycin and tetracycline hydrochloride (mix, positive controls,

448 CK^+), PDB of fungal metabolite (F-XTBG8), and bulk PDB (negative control, CK^+). The TSA plates of
449 inoculated bacterial suspension were cultured at 30°C for 12 h. The antagonistic zones (the bacterial
450 growth inhibition zone minus cup outer diameter) were measured to evaluate the antibacterial effects of F-
451 XTBG8 on different bacteria.

452 ***H. rotundifolia* genome sequencing, assembly, and annotation**

453 Genomic DNA was extracted using the QIAGEN DNaesy Plant Mini Kit and according to the
454 manufacturer's protocols. The extracted DNA molecules were sequenced by PacBio Sequel (Pacific
455 Biosciences of California, Menlo Park, CA, USA) platforms. The CLR reads were assembled using mecat2
456 (20190226) with default parameters. Draft genome was corrected by arrow and pilon. Polished contigs
457 were anchored to chromosome by Hi-C reads. First, Hi-C reads were mapped to the polished *H.*
458 *rotundifolia* genome using BWA (bwa-0.7.17) and Lachesis with default parameters (Burton et al., 2013).
459 Paired reads with mate mapped to a different contig were used to do the Hi-C associated scaffolding.
460 Lachesis was further applied to cluster, order and orient the clustered contigs. Two methods were
461 combined to identify the repeat contents in *H. rotundifolia* genome, homology-based and de novo
462 prediction. The repeat contents found by these two methods were merged by repeat masker. Protein-
463 coding genes of the *H. rotundifolia* genome were predicted by three methods, including ab initio gene
464 prediction, homology-based gene prediction and RNA-Seq-aided gene prediction (Supplementary
465 Methods 2 for genome sequencing, assembly, and annotation details).

466 ***H. rotundifolia* RNA isolation and transcriptome analysis**

467 Samples RNA were extracted using the Trizol reagent following manufacturer's recommendations
468 (Invitrogen, CA, USA) and then sequenced using the MGI-SEQ 2000 platform (Supplementary Methods 2
469 for library construction and sequencing details). Low quality reads were filtered out by SOAPnuke software
470 (Chen et al., 2017) and clean reads were mapped to *H. rotundifolia* genome using bowtie2 software
471 (Langmead 2010). Gene expression levels were estimated using FPKM values (fragments per kilobase
472 per million fragments mapped) by the RSEM software (Li and Dewey 2011). DESeq2 (Love et al., 2014)
473 was used to evaluate differential expression genes between different root samples. Genes with fold
474 change >1 or <-1, and FDR<0.05 were differential expressed genes.

475 **Statistical analysis and data normalization**

476 All data were conducted in R and visualized using the ggplot2 and igraph packages. The corrected P
477 values were used as the threshold for significantly differentially expressed genes. The microbial alpha

diversity, including the Shannon, Chao1, and Simpson indices, was determined using Mothur v. 1.34.4. The PCoA was performed to examine the similarities and dissimilarities within the different groups. Some analysis and function prediction such as Spearman's correlations, PICRUST, FUNGuild and others, were analyzed on the free online platform of the Majorbio Cloud Platform (www.majorbio.com). The base R package "stats" (v. 3.4.1) was used to perform the two-tailed Wilcoxon rank-sum test (wilcox.test function). ANOVA and mean separation using Least Significant Difference (P = 0.05) for each location. T-Test and Two-way ANOVA test were significant at P = 0.05.

Data availability

The genome, transcriptome, microbiome and other related data reported in this paper have been deposited in the National Genomics Data Center (NGDC), under accession code BioProject: PRJCA009607 (GSAs: CRA005765, https://ngdc.cncb.ac.cn/).

Acknowledgements

We would like to thank Cui Zhang (Yunnan Agricultural University) for her assistance in environmental microbes isolation experiments, and Prof. Zubin Xie (Institute of Soil Science, Chinese Academy of Sciences, CAS) and Wenjun Zhou (XTBG, CAS) for their help in nitrogen enrichment experiment. Thanks to Dr. Yu Cao (Beijing Normal University) for suggestions on data processing and article writing. We thank to Juan Guo and Shuiqing Liang (Public Technology Service Center of XTBG, CAS) for metabolites and isotopic composition analysis. We also thank the Wuhan Metware Biotechnology Co., Ltd. (Wuhan, China) and Wuhan Generead Biotechnologies Co. Ltd (Wuhan, China) for support during metabolome and genome data analysis.

Author contributions

P.X. and L.H. conceived the research and S.Z. and L.H. revised the manuscript. Z.P. completed all the sampling and measurement work. X.M. participated in the bacterial and fungal separation, nitrogen enrichment experiment, S.Z. and S.Y. contributed to the data analysis and visualization section. Z.P. and S.Z. drafted the initial version of the manuscript. All authors contributed to reviewing and finalizing the manuscript.

Funding

This study was supported by the Science and technology projects of Yunnan Province, China (No. 202003AD150007), The CAS "Light of West China" Program (xbzg-zdsys-202111) and Hainan Yazhou

Bay Seed Lab (Grant No. B21HJ0106).

Competing interests

The authors declare no competing interests.

Additional files

Additional files 1 (Supplementary Figure 1-6)

Figure S1. Aerial root mucilage (ARM) and underground root exudate (URE) compound of *H. rotundifolia*. **Figure S2**. Fungal diversity and community of aerial root mucilage (mucilage) and underground rhizosphere soil (rhizosphere). **Figure S3**. Differentiate analysis and function and phenotypic prediction of mucilage and rhizosphere bacteria. **Figure S4**. Cultured bacteria and their nitrogen-fixing capacity. **Figure S5**. Estimated genome size of *H. rotundifolia* by flow cytometry. **Figure S6**. Resistance of mucilage compound to environmental microbes. **Figure S7**. Resistance of F-XTBG8 to pathogenic and environmental fungi.

Additional files 2 (Supplementary Table 1-9)

Table S1. Relative content of different compounds and carbohydrate of aerial root mucilage (ARM) and underground root exudate (URE) **Table S2**. Fungal and bacterial OTU of different samples. **Table S3**. Differentially bacterial and fungal genera of rhizosphere and mucilage. **Table S4**. Cultured bacteria and their nitrogen-fixing capacity. **Table S5**. Plant nitrogen enrichment, length, and dry weight determination. **Table S6**. Results of plant genome sequencing, assembly, and annotation. **Table S7**. GO and KEGG enrichment of differential sample. **Table S8**. Antagonism of F-XTBG8 against different fungi and bacteria. **Table S9**. Record of mucilage production and meteorological factors. **Table S10**. Candidates for follow-up experiments in mucilage compounds. **Table S11**. The mucilage compounds for anti-microbe activity test.

Additional files 3 (Supplementary Method 1-2)

Method S1. Carbohydrate and widely targeted metabolites profiling. **Method S2.** Plant Genome and transcriptome analysis.

References

Adams, RI., Miletto, M., Taylor, JW., and Bruns, TD. (2013). Dispersal in microbes: Fungi in indoor air are dominated by outdoor air and show dispersal limitation at short distances. *The ISME Journal.* 7, 1262-1273. doi: 10.1038/ismej.2013.28

Amicucci, MJ., Galermo, AG., Guerrero, A., Treves, G., Nandita, E., Kailemia, MJ et al. (2019). Strategy for structural elucidation of polysaccharides: Elucidation of a maize mucilage that harbors diazotrophic bacteria. *Anal Chem.* 91,

7254-7265. doi: 10.1021/acs.analchem.9b00789

Bennett, AB., Pankievicz, VCS., and Ane, JM. (2020). A model for nitrogen fixation in cereal crops. *Trends Plant Sci.* 25, 226-235. doi: 10.1016/j.tplants.2019.12.004

Bloch, SE., Ryu, MH., Ozaydin, B., and Broglie, R. (2020). Harnessing atmospheric nitrogen for cereal crop production. *Current Opinion in Biotechnology.* 62, 181-188. doi: 10.1016/j.copbio.2019.09.024

Burton, JN., Adey, A., Patwardhan, RP., Qiu, R., Kitzman, JO., and Shendure, J. (2013). Chromosome-scale scaffolding of de novo genome assemblies based on chromatin interactions. *Nat Biotechnol.* 31, 1119-25. doi: 10.1038/nbt.2727

Cadot, S., Guan, H., Bigalke, M., Walser, J-C., Jander, G., Erb, M et al. (2021). Specific and conserved patterns of microbiota-structuring by maize benzoxazinoids in the field. *Microbiome.* 9, 103. doi: 10.1186/s40168-021-01049-2

Carrion, VJ., Perez-Jaramillo, J., Cordovez, V., Tracanna, V., de Hollander, M., Ruiz-Buck, D et al. (2019). Pathogen-induced activation of disease-suppressive functions in the endophytic root microbiome. *Science.* 366, 606-612. doi: 10.1126/science.aaw9285

Castrillo, G., Teixeira, PJPL., Paredes, SH., Law, TF., de Lorenzo, L., Feltcher, ME et al. (2017). Root microbiota drive direct integration of phosphate stress and immunity. *Nature.* 543, 513-518. doi: 10.1038/nature21417

Chen, S., Zhou, Y., Chen, Y., and Gu, J. (2018). Fastp: An ultra-fast all-in-one fastq preprocessor. *Bioinformatics.* 34, i884-i890. doi: 10.1093/bioinformatics/bty560

Chen, T., Nomura, K., Wang, X., Sohrabi, R., Xu, J., Yao, L et al. (2020). A plant genetic network for preventing dysbiosis in the phyllosphere. *Nature.* doi: 10.1038/s41586-020-2185-0

Chen, W., Gong, L., Guo, Z., Wang, W., Zhang, H., Liu, X et al. (2013). A novel integrated method for large-scale detection, identification, and quantification of widely targeted metabolites: Application in the study of rice metabolomics. *Mol Plant.* 6, 1769-80. doi: 10.1093/mp/sst080

Chen, Y., Chen, Y., Shi, C., Huang, Z., Zhang, Y., Li, S et al. (2017). Soapnuke: A mapreduce acceleration-supported software for integrated quality control and preprocessing of high-throughput sequencing data. *GigaScience.* 7, doi: 10.1093/gigascience/gix120

Cotton, TEA., Petriacq, P., Cameron, DD., Meselmani, MA., Schwarzenbacher, R., Rolfe, SA et al. (2019). Metabolic regulation of the maize rhizobiome by benzoxazinoids. *Isme j.* 13, 1647-1658. doi: 10.1038/s41396-019-0375-2

Dahlstrom, KM., and Newman, DK. (2022). Soil bacteria protect fungi from phenazines by acting as toxin sponges. *Current Biology.* 32, 275-288.e5. doi: https://doi.org/10.1016/j.cub.2021.11.002

Dos Santos, PC., Fang, Z., Mason, SW., Setubal, JC., and Dixon, R. (2012). Distribution of nitrogen fixation and nitrogenase-like sequences amongst microbial genomes. *BMC Genomics.* 13, 162. doi: 10.1186/1471-2164-13-162

Durán, P., Thiergart, T., Garrido-Oter, R., Agler, M., Kemen, E., Schulze-Lefert, P et al. (2018). Microbial interkingdom interactions in roots promote arabidopsis survival. *Cell.* 175, 973-983.e14. doi: 10.1016/j.cell.2018.10.020

Edgar, RC. (2013). Uparse: Highly accurate otu sequences from microbial amplicon reads. *Nat Methods.* 10, 996-8. doi: 10.1038/nmeth.2604

Eke, P., Kumar, A., Sahu, KP., Wakam, LN., Sheoran, N., Ashajyothi, M et al. (2019). Endophytic bacteria of desert cactus (euphorbia trigonas mill) confer drought tolerance and induce growth promotion in tomato (solanum lycopersicum l.). *Microbiol Res.* 228, 126302. doi: 10.1016/j.micres.2019.126302

Eskov, AK., Zhukovskaya, NV., Bystrova, EI., Orlova, YV., Antipina, VA., and Ivanov, VB. (2016). Growth of aerial roots with an extensive elongation zone by the example of a hemiepiphyte monstera deliciosa. *Russian Journal of Plant Physiology.* 63, 822-834. doi: 10.1134/s1021443716060042

Feng, Y-L., Lei, Y-B., Wang, R-F., Callaway, RM., Valiente-Banuet, A., Inderjit et al. (2009). Evolutionary tradeoffs for nitrogen allocation to photosynthesis versus cell walls in an invasive plant. 106, 1853-1856. doi: doi:10.1073/pnas.0808434106

Funk, JL., and Vitousek, PM. (2007). Resource-use efficiency and plant invasion in low-resource systems. *Nature.* 446, 1079-1081. doi: 10.1038/nature05719

Galloway, AF., Knox, P., and Krause, K. (2020). Sticky mucilages and exudates of plants: Putative microenvironmental design elements with biotechnological value. *New Phytol.* 225, 1461-1469. doi: https://doi.org/10.1111/nph.16144

Getzke, F., Thiergart, T., and Hacquard, S. (2019). Contribution of bacterial-fungal balance to plant and animal health. *Current Opinion in Microbiology.* 49, 66-72. doi: https://doi.org/10.1016/j.mib.2019.10.009

Hammerbacher, A., Coutinho, TA., and Gershenzon, J. (2019). Roles of plant volatiles in defence against microbial pathogens and microbial exploitation of volatiles. *Plant Cell Environ.* 42, 2827-2843. doi: 10.1111/pce.13602

Han, Q., Ma, Q., Chen, Y., Tian, B., Xu, L., Bai, Y et al. (2020). Variation in rhizosphere microbial communities and its association with the symbiotic efficiency of rhizobia in soybean. *The ISME Journal*. doi: 10.1038/s41396-020-0648-9

Harbort, CJ., Hashimoto, M., Inoue, H., Niu, Y., Guan, R., Rombolà, AD et al. (2020). Root-secreted coumarins and the microbiota interact to improve iron nutrition in arabidopsis. *Cell Host & Microbe.* doi: https://doi.org/10.1016/j.chom.2020.09.006

Higdon, SM., Pozzo, T., Kong, N., Huang, BC., Yang, ML., Jeannotte, R et al. (2020). Genomic characterization of a diazotrophic microbiota associated with maize aerial root mucilage. *PloS one.* 15, e0239677-e0239677. doi: 10.1371/journal.pone.0239677

Higdon, SM., Pozzo, T., Tibbett, EJ., Chiu, C., Jeannotte, R., Weimer, BC et al. (2020). Diazotrophic bacteria from maize exhibit multifaceted plant growth promotion traits in multiple hosts. *Plos One.* 15, 27. doi: 10.1371/journal.pone.0239081

Hu, L., Robert, CAM., Cadot, S., Zhang, X., Ye, M., Li, B et al. (2018). Root exudate metabolites drive plant-soil feedbacks on growth and defense by shaping the rhizosphere microbiota. *Nat Commun.* 9, 2738. doi: 10.1038/s41467-018-05122-7

Huse, SM., Dethlefsen, L., Huber, JA., Mark Welch, D., Relman, DA., and Sogin, ML. (2008). Exploring microbial diversity and taxonomy using ssu rrna hypervariable tag sequencing. *PLoS Genet.* 4, e1000255. doi: 10.1371/journal.pgen.1000255

Koprivova, A., and Kopriva, S. (2022). Plant secondary metabolites altering root microbiome composition and function. *Current Opinion in Plant Biology.* 67, doi: 10.1016/j.pbi.2022.102227

Koprivova, A., Schuck, S., Jacoby, RP., Klinkhammer, I., Welter, B., Leson, L et al. (2019). Root-specific camalexin biosynthesis controls the plant growth-promoting effects of multiple bacterial strains. *Proceedings of the National Academy of Sciences of the United States of America.* 116, 15735-15744. doi: 10.1073/pnas.1818604116

Kudjordjie, EN., Sapkota, R., Steffensen, SK., Fomsgaard, IS., and Nicolaisen, M. (2019). Maize synthesized benzoxazinoids affect the host associated microbiome. *Microbiome.* 7, 59. doi: 10.1186/s40168-019-0677-7

Langmead, B. (2010). Aligning short sequencing reads with bowtie. *Current protocols in bioinformatics.* Chapter 11, Unit 11.7. doi: 10.1002/0471250953.bi1107s32

Lebeis, SL., Paredes, SH., Lundberg, DS., Breakfield, N., Gehring, J., McDonald, M et al. (2015). Salicylic acid modulates colonization of the root microbiome by specific bacterial taxa. *Science.* 349, 860-4. doi: 10.1126/science.aaa8764

Li, B., and Dewey, CN. (2011). Rsem: Accurate transcript quantification from rna-seq data with or without a reference genome. *BMC Bioinformatics.* 12, 323. doi: 10.1186/1471-2105-12-323

Liu, X., Hu, B., and Chu, C. (2022). Nitrogen assimilation in plants: Current status and future prospects. *J Genet Genomics.* 49, 394-404. doi: 10.1016/j.jgg.2021.12.006

Liz Filartiga, A., Mantuano, D., Vieira, RC., De Toni, KLG., Vasques, GM., and Mantovani, A. (2020). Root morphophysiology changes during the habitat transition from soil to canopy of the aroid vine rhodospatha oblongata. *Ann Bot.* 127, 347-360. doi: 10.1093/aob/mcaa182 %J Annals of Botany

Love, MI., Huber, W., and Anders, S. (2014). Moderated estimation of fold change and dispersion for rna-seq data with deseq2. *Genome Biol.* 15, 550. doi: 10.1186/s13059-014-0550-8

Macabuhay, A., Arsova, B., Walker, R., Johnson, A., Watt, M., and Roessner, U. (2021). Modulators or facilitators? Roles of lipids in plant root-microbe interactions. *Trends Plant Sci.* doi: 10.1016/j.tplants.2021.08.004

Magoč, T., and Salzberg, SL. (2011). Flash: Fast length adjustment of short reads to improve genome assemblies. *Bioinformatics.* 27, 2957-63. doi: 10.1093/bioinformatics/btr507

Mohr, W., Lehnen, N., Ahmerkamp, S., Marchant, HK., Graf, JS., Tschitschko, B et al. (2021). Terrestrial-type nitrogen-fixing symbiosis between seagrass and a marine bacterium. *Nature.* doi: 10.1038/s41586-021-04063-4

Nazari, M. (2021). Plant mucilage components and their functions in the rhizosphere. *Rhizosphere.* 18, 100344. doi: https://doi.org/10.1016/j.rhisph.2021.100344

Pang, Z., Chen, J., Wang, T., Gao, C., Li, Z., Guo, L et al. (2021). Linking plant secondary metabolites and plant microbiomes: A review. *Front Plant Sci.* 12, 621276. doi: 10.3389/fpls.2021.621276

Pankievicz, VC., do Amaral, FP., Santos, KF., Agtuca, B., Xu, Y., Schueller, MJ et al. (2015). Robust biological nitrogen fixation in a model grass-bacterial association. *Plant J.* 81, 907-19. doi: 10.1111/tpj.12777

Pankievicz, VCS., Irving, TB., Maia, LGS., and Ané, JM. (2019). Are we there yet? The long walk towards the development of efficient symbiotic associations between nitrogen-fixing bacteria and non-leguminous crops. *BMC biology.* 17, 99. doi: 10.1186/s12915-019-0710-0

PIER. 2013. Pacific island ecosystems at risk. http://www.hear.org/pier/.

Pozzo, T., Higdon, SM., Pattathil, S., Hahn, MG., and Bennett, AB. (2018). Characterization of novel glycosyl hydrolases discovered by cell wall glycan directed monoclonal antibody screening and metagenome analysis of maize aerial root mucilage. *PLoS One.* 13, e0204525. doi: 10.1371/journal.pone.0204525

Randall, RP. 2012. A global compendium of weeds, second edition. A global compendium of weeds, second edition.

Sasse, J., Martinoia, E., and Northen, T. (2018). Feed your friends: Do plant exudates shape the root microbiome? *Trends Plant Sci.* 23, 25-41. doi: 10.1016/j.tplants.2017.09.003

Schütz, V., Bigler, L., Girel, S., Laschke, L., Sicker, D., and Schulz, M. (2019). Conversions of benzoxazinoids and downstream metabolites by soil microorganisms. *Frontiers in Ecology and Evolution.* 7, doi: 10.3389/fevo.2019.00238

Sharifi, R., Lee, SM., and Ryu, CM. (2018). Microbe-induced plant volatiles. *New Phytol.* 220, 684-691. doi: 10.1111/nph.14955

Shekhar, V., Stöckle, D., Thellmann, M., and Vermeer, JEM. Grossniklaus U (Ed). 2019. The role of plant root systems in evolutionary adaptation. In: Current topics in developmental biology. Academic Press.

Smith, NW., Shorten, PR., Altermann, E., Roy, NC., and McNabb, WC. (2019). The classification and evolution of bacterial cross-feeding. 7, doi: 10.3389/fevo.2019.00153

Stassen, MJJ., Hsu, S-H., Pieterse, CMJ., and Stringlis, IA. (2020). Coumarin communication along the microbiome–root–shoot axis. *Trends in Plant Science.* doi: https://doi.org/10.1016/j.tplants.2020.09.008

Stringlis, IA., Yu, K., Feussner, K., de Jonge, R., Van Bentum, S., Van Verk, MC et al. (2018). Myb72-dependent coumarin exudation shapes root microbiome assembly to promote plant health. *Proc Natl Acad Sci U S A.* 115, E5213-E5222. doi: 10.1073/pnas.1722335115

Thoms, D., Liang, Y., and Haney, CH. (2021). Maintaining symbiotic homeostasis: How do plants engage with beneficial microorganisms while at the same time restricting pathogens? 34, 462-469. doi: 10.1094/mpmi-11-20-0318-fi

Van Deynze, A., Zamora, P., Delaux, PM., Heitmann, C., Jayaraman, D., Rajasekar, S et al. (2018). Nitrogen fixation in a landrace of maize is supported by a mucilage-associated diazotrophic microbiota. *PLoS Biol.* 16, e2006352. doi: 10.1371/journal.pbio.2006352

Wolinska, KW., Vannier, N., Thiergart, T., Pickel, B., Gremmen, S., Piasecka, A et al. (2021). Tryptophan metabolism and bacterial commensals prevent fungal dysbiosis in arabidopsis roots. 118, e2111521118. doi: 10.1073/pnas.2111521118 %J Proceedings of the National Academy of Sciences

Yang, J., Lan, L., Jin, Y., Yu, N., Wang, D., and Wang, E. (2022). Mechanisms underlying legume-rhizobium symbioses. *J Integr Plant Biol.* 64, 244-267. doi: 10.1111/jipb.13207

Yu, P., He, X., Baer, M., Beirinckx, S., Tian, T., Moya, YAT et al. (2021). Plant flavones enrich rhizosphere oxalobacteraceae

669 to improve maize performance under nitrogen deprivation. *Nature Plants.* doi: 10.1038/s41477-021-00897-y
670 Zhang, W., Li, XG., Sun, K., Tang, MJ., Xu, FJ., Zhang, M et al. (2020). Mycelial network-mediated rhizobial dispersal
671 enhances legume nodulation. *ISME J.* 14, 1015-1029. doi: 10.1038/s41396-020-0587-5
672 Zotz, G., and Winkler, U. (2013). Aerial roots of epiphytic orchids: The velamen radicum and its role in water and nutrient
673 uptake. *Oecologia.* 171, 733-741. doi: 10.1007/s00442-012-2575-6
674

Supplementary Files

This is a list of supplementary files associated with this preprint. Click to download.

- Table.S5.xlsx
- Fig.S17.pdf
- SupplementalMaterial.docx
- Table.S8.xlsx
- Table.S4.xlsx
- Table.S10.xlsx
- Table.S2.xlsx
- Table.S11.xlsx
- Table.S7.xlsx
- Table.S6.xlsx
- Table.S3.xls
- Table.S1.xlsx
- Table.S9.xlsx